Forty GHz Instrument polarimeter receiver for Cosmic Microwave Background observations

Eduardo Artal Latorre(1), Enrique Villa Benito(2), Juan Luis Cano de Diego(1), Beatriz Aja Abelán(1), Luisa de la Fuente Rodríguez(1), José Vicente Terán Collantes(3), Angel Mediavilla Sánchez(1)
artale@unican.es, evilla@iac.es, juanluis.cano@unican.es, ajab@unican.es, fuenterm@unican.es, vicente.teran@erzia.com, angel.mediavilla@unican.es
(1)Departamento de Ingeniería de Comunicaciones. Universidad de Cantabria. Edificio Ingeniería de Telecomunicación. Plaza de la Ciencia s/n, 39005 Santander.
(2)now in Instituto de Astrofísica de Canarias. Calle Vía Láctea s.n. 38205 La Laguna (Tenerife)
(3)now in ERZIA Technologies. Calle Josefina de la Maza nº 4, 39012 Santander.

***Abstract*- The receiver for the Forty GHz Instrument (FGI) is a broadband microwave polarimeter to obtain three Stokes parameters (I, Q, U) of Cosmic Microwave Background waves received from the sky. The designed receiver measures I, Q, and U Stokes parameters simultaneously. This paper describes the principle of operation of the polarimeter receiver, and some details of manufactured subsystems, integration and test results. The Forty GHz Instrument is currently under installation in El Teide Observatory, Tenerife (Canary Islands), as one of the systems of QUIJOTE CMB Experiment.**

I. INTRODUCTION

The Forty GHz polarimeters for the QUIJOTE radio astronomy experiment [1] are broadband very sensitive receivers to perform scientific sky observations of the Cosmic Microwave Background (CMB). The aim of the QUIJOTE experiment is the measurement of the linear polarization percentage of the received waves from the sky. Scientific data will be used for cosmological analysis of the Universe and the indirect detection of gravitational waves. The receivers are radiometers based on cryogenically cooled front-end modules followed by room temperature back-end modules performing amplification, correlation and detection. Relative bandwidth is around 30%. The radiometers scheme is based on two balanced branches and direct detection. The Forty GHz Instrument (FGI) is a multipixel radio telescope composed of 30 identical pixels. Each pixel has an individual receiver.

II. RECEIVER SCHEME

The FGI receiver [2] is a polarimeter to obtain three (of four) Stokes parameters (I, Q, U). The Cosmic Microwave Background (CMB) is supposed to have a very weak linear polarization. The designed receiver measures the Q, U and I Stokes parameters simultaneously. The remainder Stokes parameter is V = 0, because the CMB does not have circular polarization. Stokes parameters are calculated from the incoming signal field components. A block diagram in Fig. 1 shows the configuration of the full receiver.

Each pixel of the FGI is composed of a cold Front-End Module (FEM) at 20 K, and a room temperature (298 K) Back-End Module (BEM). The cryogenic part is made up of a feedhorn, a polarizer, an Ortho-Mode Transducer (OMT) and two cryogenic low-noise amplifiers (Cryo-LNA). Outside the cryostat, two Gain and Filtering Modules, Phase Switches Module and Correlation&Detection Module operate at room temperature, in which the microwave signal is amplified, filtered, correlated by 180º microstrip hybrids and, finally, converted into DC voltages using square-law detectors. These signals are collected by a data acquisition system (DAS). The Phase Switches Modules comprise a four phase state circuit generating four polarization states. Their performance is crucial in order to obtain the Stokes parameters, minimizing the leakage among them and, at the same time, overcoming the 1/f noise and different systematic errors in the receiver. In front of the BEM, adjusting phases are located to balance the insertion phase between both branches. This adjustment must be done experimentally for each pixel in the integration and verification phase.

The connection from the FEM output to the BEM input is done by a pair of coaxial cables of the same length. Waveguide WR22 to coaxial adapters are used at FEM output and BEM input. Coaxial connectors are 2.4 mm type connectors.

III. PRINCIPLE OF OPERATION

Stokes parameters are calculated from the incoming signal field components. Using a circular basis of coordinates for the electromagnetic fields:

$$(\hat{l}, \hat{r}) \tag{1}$$

the total electric field received by the feedhorn is a combination of left hand and right hand circular electric fields:

$$\bar{E} = E_l\, \hat{l} + E_r\, \hat{r} \tag{2}$$

The electric field in rectangular coordinates is:

$$\bar{E} = E_x\, \hat{x} + j\, E_y\, \hat{y} \tag{3}$$

where these components can be expressed as

$$E_x = \frac{E_l + E_r}{\sqrt{2}} \quad ; \quad E_y = \frac{E_l - E_r}{\sqrt{2}} \tag{4}$$

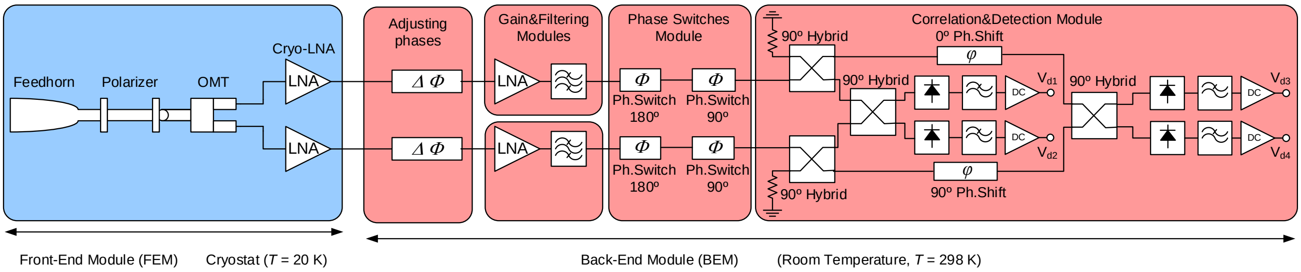

Fig. 1. Block diagram of the FGI receiver (one pixel).

The Stokes parameters I, Q and U can be obtained from left hand and right hand circular polarized components of the electric field:

$$\begin{bmatrix} I \\ Q \\ U \end{bmatrix} = \begin{bmatrix} |E_l|^2 + |E_r|^2 \\ 2\,Re(E_l^{\,*}\,E_r) \\ -2\,Im(E_l^{\,*}\,E_r) \end{bmatrix} \tag{5}$$

The combination of a 90º polarizer and the OMT give two signals at the output of the OMT. Each signal is proportional to the electric field components E_l or E_r of the total electric field received by the feedhorn antenna. In Fig. 2 there is a sketch of the signals A and B obtained at the output of the assembly feedhorn-polarizer-OMT.

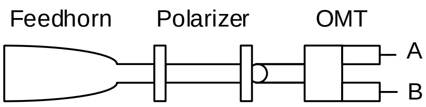

Fig. 2. OMT output signals.

A simplified block diagram of the FGI receiver is shown in Fig. 3. Front-End and Back–End amplifiers, filters and diode detectors are not included in this diagram.

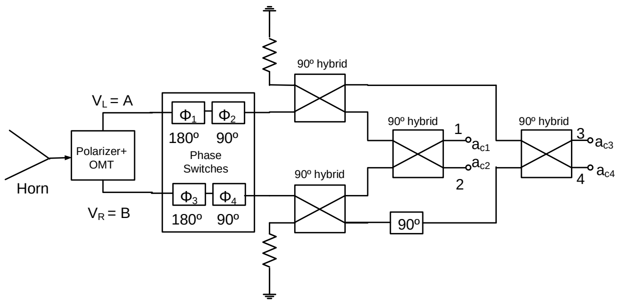

Fig. 3. Simplified block diagram of the FGI receiver.

The correlation is based on 3 dB/90º hybrids. The scheme and ports numbers for the 90º hybrid and its S-parameters are shown in Fig. 4:

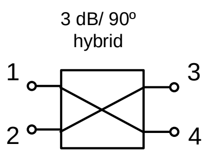

$$[S] = -\frac{1}{\sqrt{2}}\begin{bmatrix} 0 & 0 & j & 1 \\ 0 & 0 & 1 & j \\ j & 1 & 0 & 0 \\ 1 & j & 0 & 0 \end{bmatrix}$$

Fig. 4. S-parameter matrix of the 90° hybrids

Assuming as initial status a null phase in the Phase-Switches

$$\emptyset_1 = \emptyset_2 = \emptyset_3 = \emptyset_4 = 0^o \tag{6}$$

the input voltages into the Correlation&Detection Module are A and B. Solving the equations with S-parameters, the final result for the voltages at the outputs in Fig. 3 are:

$$a_{c1} = \frac{1}{2}(-A + jB) = -\frac{1}{2}(A - jB) \tag{7}$$

$$a_{c2} = \frac{1}{2}(jA - B) = \frac{1}{2}j(A + jB) \tag{8}$$

$$a_{c3} = \frac{1}{2}j(A - B) \tag{9}$$

$$a_{c4} = \frac{1}{2}(A + B) \tag{10}$$

These signals are detected by square-law Schottky diode detectors, and amplified by DC amplifiers. The signals at the BEM output are proportional to the squared amplitudes of signals in equations (7) to (10). Discarding the ½ factor, the voltage at the BEM outputs, scheme in Fig. 1, are as follows:

$$V_{d1} = |A - jB|^2 \tag{11}$$

$$V_{d2} = |A + jB|^2 \tag{12}$$

$$V_{d3} = |A - B|^2 \tag{13}$$

$$V_{d4} = |A + B|^2 \tag{14}$$

From the expression (5) the three Stokes parameters (I, Q, U) can be calculated by substitution of circular electric fields:

$$E_l = A\,;\; E_r = B \tag{15}$$

The Stokes parameters values (see Note*) are obtained as:

$$I \equiv |E_l|^2 + |E_r|^2 \;=\; |A|^2 + |B|^2$$

$$I \equiv V_{d1} + V_{d2} = V_{d3} + V_{d4} = |A + B|^2 + |A - B|^2 = |A + jB|^2 + |A - jB|^2 \tag{16}$$

$$Q \equiv 2\,Re(E_l^{\,*}\,E_r) = 2\,Re(A^*\,B)$$

$$Q \equiv V_{d4} - V_{d3} \;= |A + B|^2 - |A - B|^2 \tag{17}$$

$$U \equiv -\,2\,Im(E_l^{\,*}\,E_r) = |A + jB|^2 + |A - jB|^2$$

$$U \equiv V_{d2} - V_{d1} \;= |A + jB|^2 - |A - jB|^2 \tag{18}$$

(Note*): Stokes parameters are normalised values ranging from -1 to +1. The intensity I is always equal to +1, the expressions (16) to (18) should be normalized accordingly.

Introducing the different phase states and assuming that only the upper branch will change its phase, then:

$$\emptyset_T = \emptyset_1 + \emptyset_2 ; \qquad \emptyset_3 + \emptyset_4 = 0^o \tag{19}$$

$\emptyset_T$ is the phase difference between both receiver branches. The calculation of output voltages for the different states (0º, 90º, 180º and 270º) give the results contained in Table I.

TABLE I
OUTPUT VOLTAGES AT DIFFERENT PHASE STATES

$\emptyset_T$	0º	90º	180º	270º
V_{d1}	$\|A - jB\|^2$	$\|A - B\|^2$	$\|A + jB\|^2$	$\|A + B\|^2$
V_{d2}	$\|A + jB\|^2$	$\|A + B\|^2$	$\|A - jB\|^2$	$\|A - B\|^2$
V_{d3}	$\|A - B\|^2$	$\|A + jB\|^2$	$\|A + B\|^2$	$\|A - jB\|^2$
V_{d4}	$\|A + B\|^2$	$\|A - jB\|^2$	$\|A - B\|^2$	$\|A + jB\|^2$

Finally, the Stokes parameters calculation is made in a similar way as it is done in equations (16), (17) and (18) for the different phase states. The result is in Table II.

TABLE II
STOKES PARAMETERS AT DIFFERENT PHASE STATES

$\emptyset_T$	I	Q	U
0º	$V_{d1} + V_{d2} = V_{d3} + V_{d4}$	$V_{d4} - V_{d3}$	$V_{d2} - V_{d1}$
90º	$V_{d1} + V_{d2} = V_{d3} + V_{d4}$	$V_{d2} - V_{d1}$	$V_{d3} - V_{d4}$
180º	$V_{d1} + V_{d2} = V_{d3} + V_{d4}$	$V_{d3} - V_{d4}$	$V_{d1} - V_{d2}$
270º	$V_{d1} + V_{d2} = V_{d3} + V_{d4}$	$V_{d1} - V_{d2}$	$V_{d4} - V_{d3}$

IV. POLARIZATION COMPONENTS SEPARATION

The receiver is composed of a Front-End Module (FEM), cooled cryogenically, and a Back-End Module (BEM) operated at room temperature. The FEM contains passive waveguide components from the antenna to the input of cryogenic low-noise amplifiers (cryo-LNA): feedhorn, polarizer and OMT. A view of the FEM is depicted in Fig. 5.

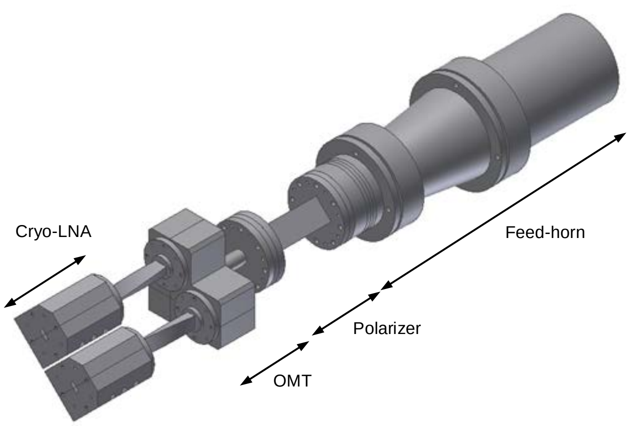

Fig. 5. Artist`s view of the Front-End Module subsystems.

The polarizer is a differential 90º phase shifter for the two orthogonal propagation modes (TE_{10} and TE_{01}) in the square waveguide. The polarizer is rotated 45º in relation to the y-axis of the feed-horn. The constant phase difference between the two modes is achieved by internal stepped ridges in the square waveguide, placed in its four internal walls. When the electric field at the polarizer input has a linear horizontal or vertical orientation (Fig. 6), each orthogonal component propagates along the ridged square waveguide with a different insertion phase. At the polarizer output the components have a 90º phase difference between them.

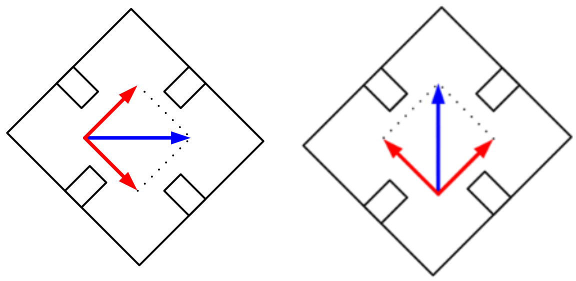

Fig. 6. Horizontal (H) and vertical (V) electric field (blue) at polarizer input. Orthogonal TE_{10} and TE_{01} components (red).

The OMT is based on a turnstile junction with an inserted scatterer. It is designed with a circular waveguide input and two WR22 rectangular waveguide in-phase outputs. The assembly polarizer-OMT (Fig. 7) has three physical ports and four electrical ports, since at the polarizer input there are two orthogonal modes. Port numbers for the S-parameters matrix are chosen as follows:

- Port #1: OMT output H
- Port #2: OMT output V
- Port #3: Polarizer input H
- Port #4: Polarizer input V

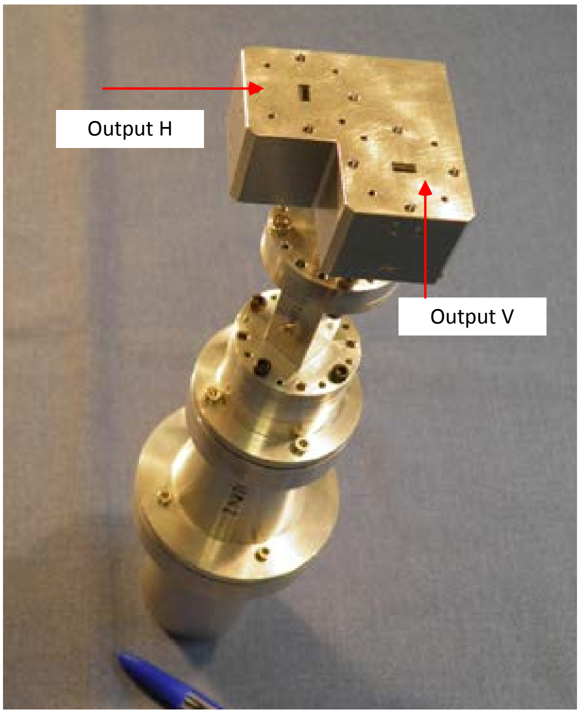

Fig. 7. Assembly Feedhorn-Polarizer-OMT.

From simulations and experimental tests of the assembly Polarizer-OMT, the ideal S-parameter matrix is:

$$[S] = \frac{1}{\sqrt{2}} \begin{bmatrix} 0 & 0 & 1 & -j \\ 0 & 0 & -j & 1 \\ 1 & -j & 0 & 0 \\ -j & 1 & 0 & 0 \end{bmatrix} \qquad (20)$$

The reference phase (0º) is taken for the transmission parameter relating the polarizer input H with the OMT output H. According to (20) with an input horizontal electric field E coming into port #3, the two OMT output signals have the same amplitude but are phase shifted by 90º. The same happens if an input vertical electric field E comes into port #4, then the two OMT output signals have the same amplitude and are phase shifted by 90º.

V. Low-Noise Amplifiers

Cryogenic LNA is based on two MMIC low-noise amplifiers on 100 nm mHEMT technology from the Fraunhofer IAF (Freiburg, Germany). The MMIC amplifier has four stages with mHEMT transistors having a 4x15 μm gate periphery. An equalizer (Fig. 8) is placed between both MMIC amplifiers to assure stability and to improve the gain versus frequency slope. The RF input and output are through WR-22 waveguide connectors.

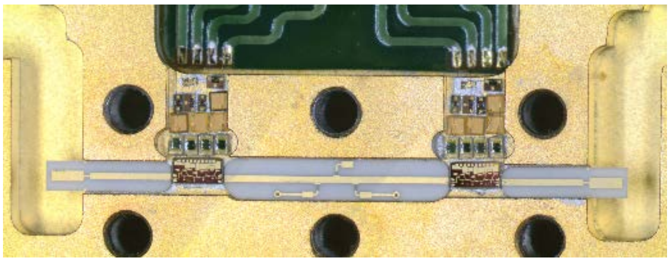

Fig. 8. Cryogenic low-noise amplifier internal view.

Typical average noise temperature of 21.3 K, with 42 dB of associated gain, have been obtained when the cryo-LNA is cooled down to 18 K.

Further amplification is done in the Back-End Module at room temperature (Fig. 1). The Gain&Filtering Module is composed of two cascaded MMIC commercial LNA, with an equalizer in-between and a microstrip filter to define the 35 to 47 GHz bandpass. Its gain is around 30 dB. A detailed view is shown in Fig. 9. This module has a positive gain slope to flatten the amplitude response of the overall receiver.

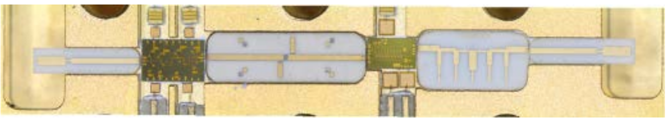

Fig. 9. BEM low-noise amplifier internal view.

VI. Phase Switches

The Phase Switches module has two separate and identical branches. Each branch has a microstrip circuit containing a power divider, a 180º phase switch, a fixed 90º differential phase shifter and a power combiner. This circuit introduces a relative phase difference of 90º, 180º and 270º by using TTL control signals. The switching devices are beam lead PIN diodes. Fig. 10 shows a view of the phase switch.

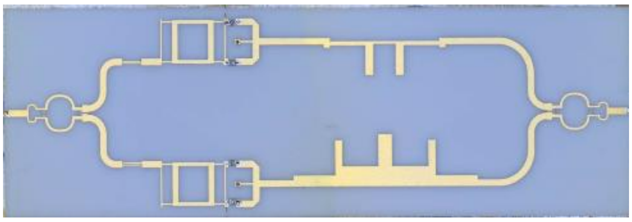

Fig. 10. Phase switch microstrip circuit.

VII. Correlation and Detection

This module consists of four hybrid couplers, a 90º phase shifter and four Schottky diode detectors. The detected signals are amplified using video amplifiers. The hybrid couplers and the phase shifter are made in rectangular waveguide. Diode detectors are manufactured in microstrip technology. An internal view detail is shown in Fig. 11.

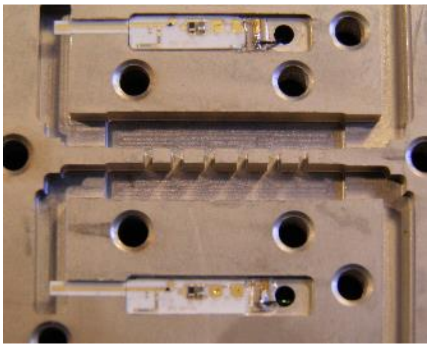

Fig. 11. Internal view detail of the Correlation-Detection Module.

The four output detected voltages are amplified by low-noise differential amplifiers.

VIII. Conclusion

The polarimeter receiver at 40 GHz for a radio astronomy instrument has been described. The principle of operation to obtain the Stokes parameters is demonstrated. Some details of the receiver subsystems have been included. The receiver is being installed in El Teide Observatory (Tenerife).

Acknowledgements

The authors would like to thank the Spanish Ministry of Economy and Competitiveness for the financial support through Consolider-Ingenio 2010 program grant CSD2010-00064 and under the grant ESP2015-70646-C2-2-R. The authors would also like to thank Eva María Cuerno for the circuits fabrication and integration.

References

[1] M. R. Pérez-de-Taoro et alt. “QUIJOTE Experiment: status of telescopes and instrumentation”, Proc. SPIE 9906, Ground-based and Airborne Telescopes VI, 99061K (27 July 2016).

[2] E. Villa, J. L. Cano, B. Aja, J.V. Terán, L. de la Fuente, A. Mediavilla, E. Artal, “Polarimetric receiver in the forty gigahertz band: new instrument for the Q-U-I joint Tenerife experiment”. Experimental Astronomy (2018) 45:127–146